



Synthesis of Fe₃O₄-supported Schiff base Cu (II) complex: a novel efficient and recyclable magnetic nanocatalyst for one-pot three-component synthesis of quinolin-5-one, chromene-3-carbonitrile and phthalazine-5,10-dione derivatives

Hakimeh Ebrahimiasl¹ · Davood Azarifar¹ · Mahsa Mohammadi^{1,2,3} · Hassan Keypour¹ · Masoumeh Mahmood abadi¹

Received: 4 August 2020 / Accepted: 3 October 2020
© Springer Nature B.V. 2020

Abstract

In this research, synthesis and characterization of a novel Schiff base Cu (II) complex immobilized on Fe₃O₄@SiO₂ nanoparticles are reported. Then, the catalytic activity of these nanoparticles as magnetic recyclable nanocatalyst was explored for the one-pot three-component synthesis of quinolin-5-one, chromene-3-carbonitrile and phthalazine-5,10-dione derivatives. The reactions proceeded smoothly to provide the respective products in excellent yields under green conditions. Facile preparation of the catalyst, high yields of the products, low reaction times, and use of water as green solvent are the main advantages of the present protocol. Moreover, the catalyst can be easily separated from the reaction mixture in a magnetic field, recycled and reused for six consecutive fresh runs without considerable loss of catalytic activity.

Electronic supplementary material The online version of this article (<https://doi.org/10.1007/s11164-020-04293-7>) contains supplementary material, which is available to authorized users.

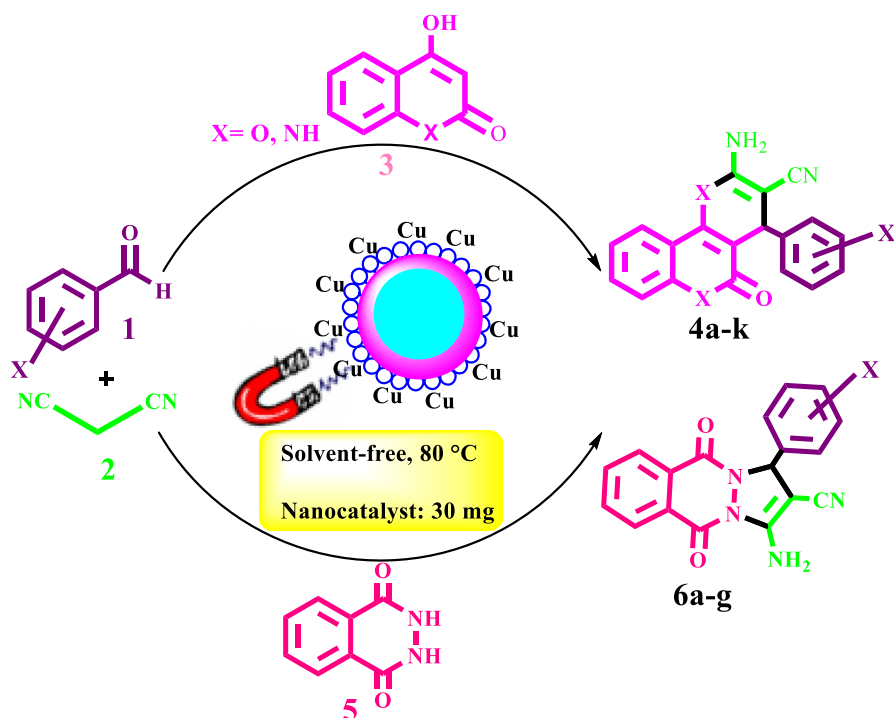
✉ Hakimeh Ebrahimiasl
h_ebrahimiasl64@yahoo.com

¹ Department of Chemistry, Bu-Ali Sina University, 65178 Hamedan, Iran

² Pharmaceutical Sciences Research Center, School of Pharmacy, Health Institute, Kermanshah University of Medical Sciences, Kermanshah, Iran

³ Department of Medicinal Chemistry, Faculty of Pharmacy, Kermanshah University of Medical Sciences, Kermanshah, Iran

Graphic abstract



Keywords Fe₃O₄-supported cu (II) Schiff-base complex · Magnetic nanoparticles · Multicomponent reaction · Quinolin-5-one · Chromene-3-carbonitrile · Phthalazine-5,10-dione

Introduction

In chemistry, quite often, ligands include with a ring size of nine or more atoms (containing hetero atoms) and contain at least three donor sites [1]. So far, a variety of synthetic and natural compounds such as crown ethers, Schiff bases and porphyrins have been investigated [2]. Several compounds and their derivatives exhibit high affinity for metal ions and host various neutral molecules and organic cation guests and are also useful in phase transfer catalysis and biological studies [3, 4]. In recent years, the chemistry of transition metal ion-based complexes of ligands has attracted enormous interest in the field of coordination chemistry [5–7]. Many transition metals prompted Schiff base complexes have been reported to perform the excellent catalytic activity in various homogeneous and heterogeneous reactions [8]. However, these Schiff base complexes generally suffer from certain drawbacks including instability, expensive and tedious purification steps, inefficient recycling

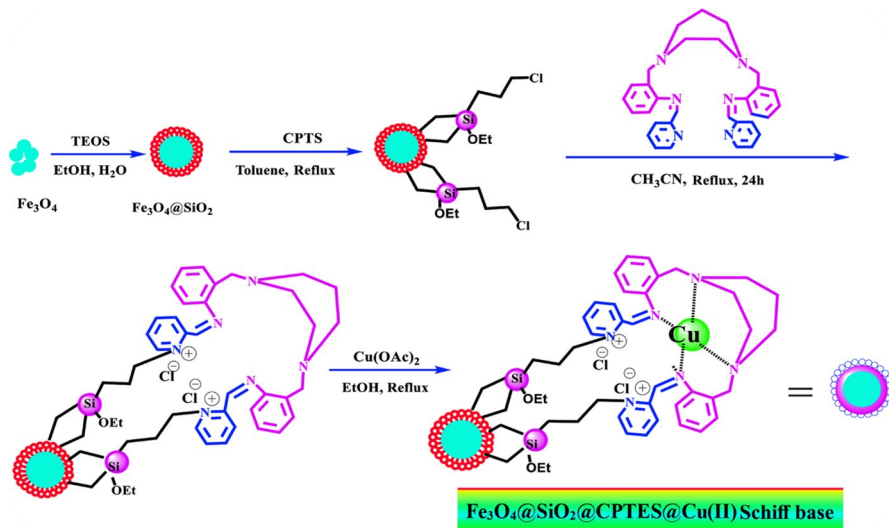
and reusability. One recently emerged useful strategy to overcome these drawbacks is the immobilization of Schiff base complexes and other homogeneous catalysts onto different support materials such as inorganic silica, organic polymers and nano-sized metal oxides [9, 10]. The immobilization incorporates all the advantages of both heterogeneous and homogeneous catalysts to provide the catalysts with highly improved stability and catalytic activity [9]. Among the frequently used nano-supports, magnetic nanoparticles (MNPs) have emerged as excellent candidates because of their heterogeneous and magnetic nature, high surface area, environmental benignity, facile magnetic separation and efficient recyclability [11–14].

Schiff bases are well-reported compounds carrying imine or azomethine (C=N) functional group and form an important class of the most widely used organic compounds [15, 16]. Schiff bases have gained growing importance due to their broad spectrum of biological activities and wide applications in many different fields including medicinal, pharmaceutical, analytical, and inorganic chemistry [17–19]. Besides, Schiff bases are used as catalysts, intermediates in organic synthesis and the preparation of several industrial products like dyes, pigments, polymer stabilizers [16], and corrosion inhibitors [20]. Within the last few decades, several transition metal Schiff base complexes have been synthesized and their importance in biochemical, catalytic and industrial processes has been widely investigated [1, 2, 21–27]. Moreover, transition metal Schiff base complexes have gained enormous interest owing to their biological activities as anticarcinogenic, antiviral [28], antifertile [29], antifungal and antibacterial agents [30]. Many different Cu (II) Schiff base complexes, such as Cu (II) isatin Schiff base complexes, have been known as potential antitumor agents [31]. Among several transition metals vitally important to the chemistry of living systems, copper is by far the most familiar and widespread example which performs an important biological function in living organisms and found in plants and numerous proteins. Moreover, a large number of nanoparticles based on the earth-abundant and inexpensive copper metal have found wide applications in the field of catalysis due to their interesting features including low price, facile separation and high catalytic performance [32, 33]. Copper complexes immobilized on Fe₃O₄ nanoparticles have exhibited high catalytic performance for a wide range of organic transformations like oxidation, C–C coupling and condensation reactions [34–37]. A variety of Cu complexes supported on the magnetic nanoparticles as catalysts such as γ -Fe₂O₃–Cu-complex [38], Cu-SPATB/Fe₃O₄ [39], Cu/imine@Fe₃O₄ MNPs [40], and Cu-HB@AS-MNPs [41] have been reported in the literature. Based on these reports, it is understood that a new window has been opened on the Fe₃O₄-supported Schiff base complexes of Cu as catalysts in one-pot multicomponent reactions. Multicomponent reactions (MCRs) have gained enormous interest as an especially useful synthetic strategy with high diversity in the reactions combining economic aspects with environmental anxiety [42]. MCRs involve two or more steps that accomplish by successive reactions between three or more reactants without separation of the intermediates. As a result, the MCRs benefit from several advantages such as waste prevention, atom-economy, energy efficiency, yield improvement, and short reaction times [43].

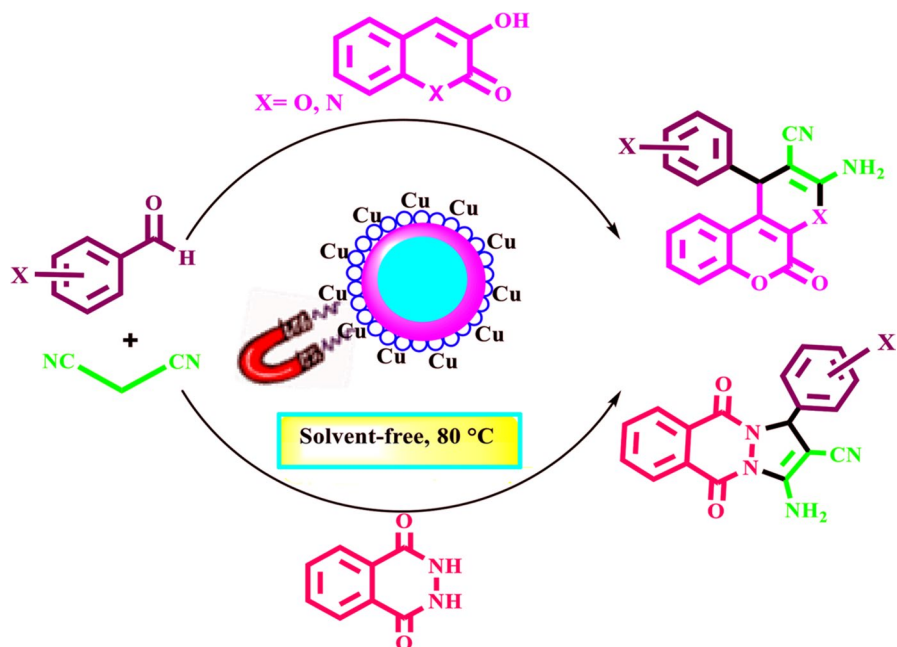
In the last few decades, the one-pot multicomponent reactions have found wide applications in synthetic chemistry particularly for the synthesis of a wide variety

of biologically active heterocyclic compounds [44]. The most frequently used therapeutic pharmaceuticals worldwide contain certain heterocyclic scaffolds as the key structural units. Among the heterocyclic compounds of biological importance, coumarin, pyrroloquinoline and phthalazine nucleus are of considerable significance owing to their presence in biologically active compounds, pharmaceuticals, the broad range of natural products and functional materials [45–48].

Considering the broad range applications of the coumarin, pyrroloquinoline and phthalazine derivatives, a great interest has been focused on the development of more efficient and eco-friendly protocols for the synthesis of these compounds. This prompted us to synthesis a novel nanomagnetic copper (II) complex using Schiff base ligand as a heterogeneous and reusable catalyst in the synthesis of organic compounds. In continuation of our research program in developing more efficient and recyclable catalysts and, also environmentally friendly protocols for the synthesis of heterocyclic compounds, herein, we report the design, synthesis and characterization of the Schiff base Cu (II) complex immobilized on the surface of $\text{Fe}_3\text{O}_4/\text{SiO}_2$ MNPs (Scheme 1) and its application as a reusable nanocatalyst for one-pot three-component and solvent-free synthesis of [3,2-*c*]quinolin-5-one, [3,2-*c*]chromene-3-carbonitrile and [1,2-*b*]phthalazine-5,10-dione derivatives (Scheme 2). Also, thanks to facile synthesis of catalyst support, easy accessibility and low price of copper (Cu) source, we were able to synthesize this new nanocatalyst on a large scale.



Scheme 1 Immobilization process of Schiff base and its Cu(II) complex on $\text{Fe}_3\text{O}_4/\text{SiO}_2$



Scheme 2 Three-component synthesis of various [3,2-*c*]quinolin-5-one, [3,2-*c*]chromene-3-carbonitrile and [1,2-*b*]phthalazine-5,10-dione derivatives catalyzed by $\text{Fe}_3\text{O}_4@ \text{SiO}_2@ \text{CPTES} @ \text{Cu(II)}$ Schiff base complex MNPs

Experimental

Materials

Starting materials and used solvents were purchased from Merck Chemical Company and used without further purification.

Characterization techniques

Melting points were determined in open capillary tubes using a BUCHI 510 apparatus. Fourier transform infrared (FT-IR) spectra were recorded from KBr pellets on a PerkinElmer GX FT-IR spectrometer. ¹H NMR and ¹³C NMR spectra were recorded for samples in DMSO-*d*₆ on 90, 400 and 500 MHz Bruker Avance instruments at ambient temperature using tetramethylsilane (TMS) as the internal standard. Scanning electron microscopy (SEM) images were obtained on EM3200 instrument operated at 30 kV accelerating voltage. Energy-dispersive X-ray (EDX) analysis was carried out using a FESEM-SIGM (German) instrument. The curves obtained from thermo-gravimetric analysis (TGA) were recorded in the air using TGA/DTA Pyris Diamond instrument. Magnetic measurement of the catalyst was taken using a vibrating sample magnetometer (VSM) instrument MDKFT. Moreover, transmission

electron microscopy (TEM) was performed using a Zeiss-EM10C-100kv CM30, (300KV) instrument. Wavelength- dispersive X-ray spectroscopy (WDX) was performed using a TESCAN mira3. Inductively coupled plasma optical emission spectroscopy (ICP-OES) was performed by Arcos EOP, 32 Linear CCD simultaneous ICP analyzer.

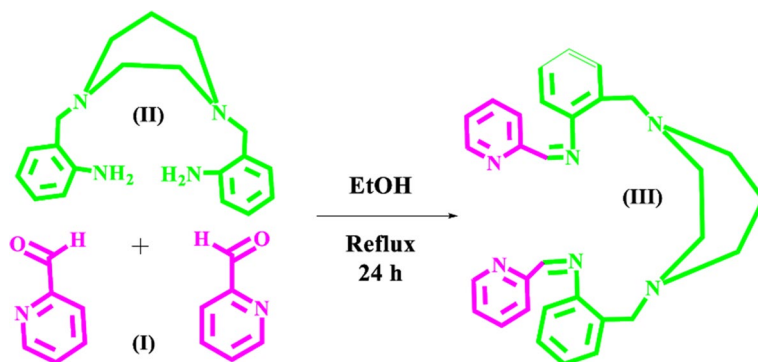
Synthesis

Synthesis of the Schiff base ligand (III)

For the synthesis of the Schiff base ligand (III), 2-((4-(2-aminobenzyl)-1,4-diazepan-1-yl)methyl)benzenamine (0.31 g, 1 mmol) dissolved in ethanol (20 mL) was added dropwise with stirring to a solution of 2-Pyridinecarboxaldehyde (0.2 g, 2 mmol) in ethanol (20 mL) (Scheme 3) [49]. The mixture was stirred and refluxed for 24 h. After the completion of the reaction, the orange Schiff base (III) was recovered by simple filtration and then repeatedly washed with cold methanol, and dried in vacuum to yield the desired product (Scheme 2). Yield: 0.26 g (86%). M.p: 112 °C. Anal. Calc. for $C_{31}H_{32}N_6$ (M. W: 488.27): C, 76.20; H, 6.60; N, 17.20. Found: C, 76.32; H, 6.45; N, 17.33%. EI-MS (m/z): 488.27. IR (KBr, cm^{-1}) ν : 1628 (C=N), 1606, 1587 [(C=C) and (C=N)_{py}]. 1H NMR (DMSO- d_6 , ppm) δ_c : 1.762–1.795 (m, 2H_a), 2.708–2.727 (t, 4H_b), 3.595–3.609 (d, 4H_c), 3.812 (s, 4H_d), 6.940–8.260 (m, 16H_{Aro}), 8.515 (s, 2H_k). ^{13}C NMR (DMSO- d_6 , ppm) δ_c : 27.5 (C_a), 56.7 (C_b), 59.71 (C_c), 59.13(C_d), 118.47–149.1 (C_{Aro}), 151.9 (C_k).

Synthesis of the Fe_3O_4 and $Fe_3O_4@SiO_2$

Nano-magnetic Fe_3O_4 were prepared by co-precipitation of Fe^{3+} and Fe^{2+} ions with $[Fe^{3+}]/[Fe^{2+}]$ molar ratio of 2:1 as described according to the reported method [50]. Briefly, $FeCl_3 \cdot 6H_2O$ (5.4 g, 0.02 mol) and $FeCl_2 \cdot 4H_2O$ (2.0 g, 0.01 mol) were stirring and dissolved in deionized water (80 mL) under N_2 flow and vigorous stirring



Scheme 3 Synthesis of the Schiff base ligand (III)

conditions. Then a solution of NH₄OH (25%, 15 mL) was rapidly added to the mixture at 80 °C to form black Fe₃O₄ magnetic nanoparticles. The Fe₃O₄ NPs were filtered and washed several times with H₂O and EtOH and at the end stored in a vacuum desiccator at 4 °C for using in further. The Fe₃O₄@SiO₂ were prepared according to the Stober method [51]. Fe₃O₄ particles (100 mg) were suspended in a mixture of 100 mL of ethanol 10 mL of deionized water in (25 mL) round-bottom flask and then tetraethyl orthosilicate (TEOS) was dispersed in the reaction mixture and stirred for 2 h at room temperature to facilitate TEOS coating. The dark-brown precipitate was separated using a magnet and washed several times with ethanol to afford the desired product.

Synthesis of the Fe₃O₄@SiO₂@CPTES

To form Fe₃O₄@SiO₂@CPTES, Fe₃O₄@SiO₂ was modified with 3-chloropropyltriethoxysilane (CPTES) [52]. In short, 100 mg of the Fe₃O₄@SiO₂ was added to dry toluene (100 mL) in a round-bottom flask and then to CPTES (3 mL) was put in the reaction under N₂ atmosphere and stirred at 90 °C for 12 h. The product (Fe₃O₄@SiO₂@CPTES) was obtained by separation with a magnet and washed with toluene three times and stored for further use.

Synthesis of the Fe₃O₄@SiO₂@CPTES@ Schiff base

Functionalization of Fe₃O₄@SiO₂@CPTES was performed by a Schiff base ligand (III). In brief, for the synthesis of Fe₃O₄@SiO₂@CPTES@ Schiff base, the Fe₃O₄@SiO₂@CPTES (100 mg) was dispersed in CH₃CN (25 mL). Then, a solution of the Schiff base ligand (III) (1 mmol) in acetonitrile (5 mL) was added to a mixture of the Fe₃O₄@SiO₂@CPTES and refluxed for 24 h under N₂. Ultimately, the Fe₃O₄@SiO₂@CPTES@ Schiff base was separated with an external magnet and washed with acetonitrile 3 times until the product obtained and dried under vacuum for 24 h.

Synthesis of the Fe₃O₄@SiO₂@CPTES@Cu(II) Schiff base complex NPs

Fe₃O₄@SiO₂@CPTES@Cu(II) Schiff base complex NPs were prepared by using a simple reflux method. The dissolved solution of Cu(OAc)₂ (5% (w/v)) in ethanol (5 mL) was slowly added to the Fe₃O₄@SiO₂@CPTES@ Schiff base (50 mg) solution in ethanol (20 mL) under constant stirring and refluxed for 24 h. The obtained product was washed with ethanol to remove unreacted Cu(OAc)₂ and dried in a vacuum oven at 60 °C for 5 h (Scheme 1).

Overall template synthesis of dihydropyrano[3,2-c]chromen-2-one, 2-amino-3-cyano-1,4,5,6-tetrahydropyrano[3,2-c]quinolin-5-one and 1H-pyrazolo[1,2-b]phthalazine-5,10-diones derivatives

A mixture of aromatic aldehyde (1 mmol), malononitrile (1 mmol), 4-hydroxycoumarin/4-hydroxyquinolin-2(1H)-one/ phthalhydrazide (1 mmol)

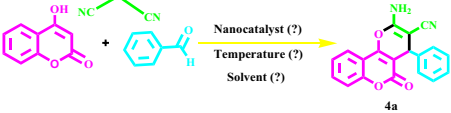
and nano-catalyst (30 mg) was stirred at 80 °C under the solvent-free condition for 10–15 min (Scheme 3). After completion (by TLC), the resulting solid was diluted with hot ethanol (5 mL) and the catalyst was isolated by an external magnet. The obtained precipitate was purified by simple recrystallization in EtOH to yield the pure product. The structures of the products were established on their melting points and spectral (FT-IR, ^1H NMR and ^{13}C NMR) analysis and compared with the reported data (Tables 1 and 2). The structure of the synthesized products was confirmed by ^1H NMR, ^{13}C NMR and IR (Supporting Information).

Spectral selected data

2-Amino-4,5-dihydro-4-(4-hydroxyphenyl)-5-oxopyrano[3,2-c]chromene-3-carbonitrile (4b)

Cream solid; m.p. 262–264 °C; IR (KBr) ($\nu_{\text{max}}/\text{cm}^{-1}$): 3504, 3407, 3283, 2196, 1696, 1673, 1609 cm^{-1} ; H-NMR (90 MHz, DMSO- d_6) δ : 4.31 (s, 1H, C-H), 6.62–7.91 (m, 10H, H-Ar and NH2), 9.34 (s, 1H, O-H) ppm.

Table 1 Optimization reaction for the synthesis of 2-amino-5-oxo-4-phenyl-4*H*,5*H*dihydropyrano[3,2-*c*]chromene-3-carbonitrile derivatives



Entry	Catalyst amount (mg)	Solvent	Temperature (°C)	Time (min)	Yield ^a
1	No catalyst	H ₂ O	25	120	–
2	0.01	H ₂ O	25	120	30
3	0.01	EtOH	25	90	32
4	0.01	CH ₃ CN	25	60	50
5	0.01	Solvent-Free	25	50	58
6	0.01	H ₂ O	Reflux	60	45
7	0.01	EtOH	Reflux	60	62
8	0.01	CH ₃ CN	Reflux	60	68
9	0.01	Solvent-free	70	40	72
10	0.01	Solvent-free	100	40	75
11	0.02	Solvent-free	80	15	97
12	0.03	Solvent-free	80	10	98
13	0.04	Solvent-free	70	10	85

Reaction Condition: benzaldehyde (1 mmol), 4-hydroxycoumarin (1 mmol), malononitrile (1 mmol), solvent (5 ml), ^aIsolated yields

Table 2 Fe₃O₄@SiO₂@CPTES@Cu (II) Schiff base complex catalyzed synthesis of synthesis of 5-oxo-dihydropyrano[3,2-*c*]chromene and 2-amino-3-cyano-1,4,5,6-tetrahydropyrano[3,2-*c*]quinolin-5-one derivatives

Nanocatalyst: 30 mg
Solvent-free, 80 °C

Entry	R	X	Product	Time (min)	Yield ^b (%)	M.P (°C) [Lit.] [53–58]
1	H	O		10	98	252–254
2	4-OH	O		15	90	262–264
3	4-OCH ₃	O		15	89	240–242
4	4-CH ₃	O		15	92	250–252
5	2-Cl	O		10	97	260–262
6	2-NO ₂	O		10	97	252–254
7	4-Br	O		10	96	255–257
8	2,4-Cl ₂	O		10	97	254–256

Table 2 (continued)

Entry	R	X	Product	Time (min)	Yield ^b (%)	M.P (°C) [Lit.] [53–58]
9	H	NH		10	96	> 300
10	4-CH ₃	NH		15	90	> 300
11	4-Br	NH		10	97	> 300

Conditions: aldehyde (1 mmol), malononitrile (1 mmol), 4-hydroxycoumarin/4-hydroxyquinolin-2(1*H*)-one (1 mmol), catalyst (30 mg), 80 °C, ^aIsolated pure yield

2-Amino-4,5-dihydro-4-(4-methoxyphenyl)-5-oxopyrano[3,2-*c*]chromene-3-carbonitrile (**4c**)

Cream solid; m.p. 240–242 °C; IR (KBr) (ν_{\max} /cm⁻¹): 3389, 3293, 2195, 1715, 1676, 1605 cm⁻¹; ¹H-NMR (90 MHz, DMSO-*d*₆) δ : 4.70 (s, 1H, C-H), 6.78–7.94 (m, 10H, H-Ar and NH₂), 3.70 (s, 3H, OCH₃) ppm.

2-Amino-4-(2-chlorophenyl)-4,5-dihydro-5-oxopyrano[3,2-*c*]chromene-3-carbonitrile (**4e**)

Cream solid; m.p. 260–262 °C; IR (KBr) (ν_{\max} /cm⁻¹): 3407, 3324, 2192, 1711, 1608, 1528 cm⁻¹; ¹H-NMR (400 MHz, DMSO-*d*₆) δ : 4.98 (s, 1H, C-H), 7.35–7.92 (m, 10H, H-Ar and NH₂) ppm; ¹³C-NMR (400 MHz, DMSO-*d*₆) δ : 36.4, 56.6, 103.1, 112.8, 116.5, 118.6, 122.5, 122.8, 124.6, 128.2, 129.0, 130.6, 132.7, 133.0, 135.5, 152.1, 153.9, 158.0, 159.3 ppm.

2-Amino-4,5-dihydro-4-(2-nitrophenyl)-5-oxopyrano[3,2-c]chromene-3-carbonitrile (4f)

Cream solid; m.p. 252–254 °C; IR (KBr) ($\nu_{\max}/\text{cm}^{-1}$): 3401, 3312, 2193, 1702, 1674, 1607 cm^{-1} ; ¹H-NMR (90 MHz, DMSO-d₆) δ : 5.23 (s, 1H, C-H), 7.56–8.00 (m, 10H, H-Ar and NH₂) ppm.

2-Amino-4-(4-bromophenyl)-4,5-dihydro-5-oxopyrano[3,2-c]chromene-3-carbonitrile (4 g)

Cream solid; m.p. 255–257 °C; IR (KBr) ($\nu_{\max}/\text{cm}^{-1}$): 3386, 3312, 3187, 2191, 1716, 1676, 1608; ¹H-NMR (400 MHz, DMSO-d₆) δ : 4.5 (s, 1H, C-H), 7.28–7.91 (m, 10H, Ar-H and NH₂) ppm; ¹³C NMR (100 MHz, DMSO-d₆) δ 34.3, 56.4, 102.9, 103.3, 117.1, 119.3, 123.01, 125.2, 128.3, 129.3, 132.6, 133.6, 133.8, 139.9, 152.7, 154.6, 158.5, 158.4, 159.9 ppm.

2-Amino-4-(2,4-dichlorophenyl)-4,5-dihydro-5-oxopyrano[3,2-c]chromene-3-carbonitrile (4 h)

Cream solid; m.p. 254–256 °C; IR (KBr) ($\nu_{\max}/\text{cm}^{-1}$): 3460, 3294, 2200, 1716, 1674, 1630 cm^{-1} ; ¹H-NMR (400 MHz, DMSO-d₆) δ : 4.98 (s, 1H, C-H), 7.35–7.92 (m, 9H, H-Ar and NH₂) ppm; ¹³C-NMR (100 MHz, DMSO-d₆) δ : 34.3, 56.4, 102.9, 113.3, 114.1, 119.1, 123.0, 125.2, 128.3, 129.3, 132.5, 132.8, 133.6, 133.8, 139.9, 152.9, 154.6, 158.5, 158.6, 159.9 ppm.

2-Amino-5,6-dihydro-5-oxo-4-p-tolyl-4H-pyrano[3,2-c]quinoline-3-carbonitrile (4j)

Pale yellow powder; mp > 300; IR (KBr) ($\nu_{\max}/\text{cm}^{-1}$): 3410, 3284, 3163, 2189, 1668, 1384, 1365 cm^{-1} ; ¹H-NMR (500 MHz, DMSO-d₆) δ : 2.24 (s, 3H, C-H), 4.44 (s, 1H, C-H), 7.08 (s, 4H, H-Ar), 7.23 (s, 2H, NH₂), 7.25–7.38 (m, 2H, H-Ar), 7.58 (t, J = 7.7 Hz, 1H, H-Ar), 7.90 (d, J = 7.9 Hz, 1H, H-Ar), 11.76 (s, 1H, NH) ppm; ¹³C NMR (125 MHz, DMSO-d₆) δ : 21.0, 36.7, 58.4, 110.2, 112.5, 115.7, 120.2, 122.2, 122.3, 127.7, 129.3, 131.5, 136.2, 138.2, 141.8, 151.5, 159.4, 160.9 ppm.

2-Amino-4-(4-bromophenyl)-5,6-dihydro-5-oxo-4H-pyrano[3,2-c]quinoline-3-carbonitrile (4 k)

Pale yellow powder; mp > 300 °C; IR (KBr) ($\nu_{\max}/\text{cm}^{-1}$): 3404, 3287, 3173, 2188, 1672, 1321, 1379 cm^{-1} ; ¹H-NMR (500 MHz, DMSO-d₆) δ : 4.49 (s, 1H, C-H), 7.17 (d, J = 8.4 Hz, 4H, H-Ar), 7.28–7.35 (s, 2H NH₂), 7.47 (d, J = 8.4 Hz, 2H, H-Ar), 7.60 (t, J = 16.4, 8.2 Hz, 1H, H-Ar), 7.91 (d, J = 7.9 Hz, 1H, H-Ar), 11.80 (s, 1H, NH) ppm; ¹³C NMR (125 MHz, DMSO-d₆) δ : 36.7, 57.7, 109.4, 112.3, 115.8, 120.0, 120.2, 122.2, 122.4, 130.1, 131.6, 131.7, 138.3, 144.2, 151.7, 159.3, 160.8 ppm.

3-Amino-5,10-dihydro-5,10-dioxo-1-phenyl-1H-pyrazolo[1,2-b]phthalazine-2-carbonitrile (6a)

Yellow solid; m.p. 272–274 °C; IR (KBr) ($\nu_{\max}/\text{cm}^{-1}$): 3361, 3316, 2197, 1682, 1660 cm^{-1} ; $^1\text{H-NMR}$ (90 MHz, DMSO- d_6) δ : 6.12 (s, 1H, C-H), 7.37–8.00 (m, 11H, H-Ar and NH_2) ppm; $^{13}\text{C NMR}$ (100 MHz, DMSO- d_6) δ : 39.5, 61.4, 62.9, 116.0, 126.6, 138.4, 150.6, 153.6, 156.6 ppm.

3-Amino-5,10-dihydro-5,10-dioxo-1-p-tolyl-1H-pyrazolo[1,2-b]phthalazine-2-carbonitrile (6b)

Yellow solid; m.p. 256–258 °C; IR (KBr) ($\nu_{\max}/\text{cm}^{-1}$): 3363, 3262, 2197, 1656, 1567 cm^{-1} ; $^1\text{H-NMR}$ (90 MHz, DMSO- d_6) δ : 2.28 (s, 3H, C-H), 6.08 (s, 1H, C-H), 7.10–8.20 (m, 10H, H-Ar and NH_2) ppm.

3-Amino-5,10-dihydro-1-(4-methoxyphenyl)-5,10-dioxo-1H-pyrazolo[1,2-b]phthalazine-2-carbo-nitrile (6c)

Yellow solid; m.p. 240–242 °C; IR (KBr) ($\nu_{\max}/\text{cm}^{-1}$): 3376, 3308, 2197, 1677, 1661 cm^{-1} ; $^1\text{H-NMR}$ (400 MHz, DMSO- d_6) δ : 3.80 (s, 3H, OCH_3), 6.15 (s, 1H, CH), 6.95–8.31 (m, 10H, H-Ar and NH_2) ppm, $^{13}\text{C NMR}$ (100 MHz, DMSO- d_6) δ : 55.1, 61.3, 62.6, 113.8, 116.1, 125.1, 126.6, 127.2, 128.5, 128.7, 130.1, 132.5, 133.7, 134.6, 150.6, 153.6, 156.6, 159.2 ppm.

3-Amino-1-(2,4-dichlorophenyl)-5,10-dihydro-5,10-dioxo-1H-pyrazolo[1,2-b]phthalazine-2-carbo-nitrile (6d)

Yellow solid; m.p. 246–248 °C; IR (KBr) ($\nu_{\max}/\text{cm}^{-1}$): 3370, 3360, 2204, 1676, 1632 cm^{-1} ; $^1\text{H-NMR}$ (400 MHz, DMSO- d_6) δ : 6.48 (s, 1H, CH), 7.35–8.27 (m, 9H, H-Ar and NH_2) ppm, $^{13}\text{C NMR}$ (100 MHz, DMSO- d_6) δ : 39.5, 59.7, 60.6, 116.0, 125.5, 135.2, 151.7, 154.0, 157.1 ppm.

3-Amino-5,10-dihydro-5,10-dioxo-1-(pyridin-4-yl)-1H-pyrazolo[1,2-b]phthalazine-2-carbonitrile (4f)

Yellow solid; m.p. 260–262 °C; IR (KBr) ($\nu_{\max}/\text{cm}^{-1}$): 3388, 3285, 2198, 1681, 1664, 1604, 1579 cm^{-1} ; $^1\text{H-NMR}$ (400 MHz, DMSO- d_6) δ : 6.21 (s, 1H, CH), 7.57–8.64 (m, 10H, H-Ar and NH_2) ppm, $^{13}\text{C NMR}$ (100 MHz, DMSO- d_6) δ : 60.1, 61.7, 115.7, 121.3, 126.7, 127.2, 128.3, 128.9, 133.8, 134.6, 147.1, 149.9, 150.9, 153.7, 156.7 ppm.

Results and discussion

Preparation of the novel copper(II) complexes using Schiff base ligand-coated Fe₃O₄ nanoparticles as catalyst

Herein, we report the stepwise synthesis of hitherto unexplored Fe₃O₄-supported copper (II) Schiff base complex Fe₃O₄@SiO₂@CPTES@Cu(II) Schiff base complex NPs as an efficient and recyclable heterogeneous nano-catalyst as explained above (Scheme 1). In first, preparation of the Schiff base ligand (II) is similar to the reported method [20] (Scheme 2). Then, the silica-coated Fe₃O₄ MNPs were prepared by co-precipitation of ferrous (Fe²⁺) and ferric (Fe³⁺) ions followed by the reaction of dispersion of the resulted nanoparticles in ethanol and deionized water with tetraethyl orthosilicate (TEOS) in the presence of 25% ammonia solution to obtain the core-shell Fe₃O₄@SiO₂ nanoparticles. In the next step, the Fe₃O₄@SiO₂ nanoparticles were reacted with (3-chloropropyl)triethoxysilane (CPTES) in dry toluene under nitrogen atmosphere to obtain the chloro-functionalized Fe₃O₄@SiO₂@CPTES MNPs. Then, the reaction of Fe₃O₄@SiO₂-(CH₂)₃-Cl nanoparticles with Schiff base ligand (II) in acetonitrile containing few drops of triethylamine under a nitrogen atmosphere and refluxed condition furnished the Fe₃O₄@SiO₂@CPTES@ Schiff base nanoparticles. In the last step, copper (II) was supported on the surface of Schiff- base-modified magnetic nanoparticles via reaction with Cu(OAc)₂ in ethanol under reflux conditions.

Characterization of the catalyst Fe₃O₄@SiO₂@CPTES@Cu (II) Schiff base complex NPs

Spectral measurements including FT-IR, XRD, SEM, TEM, EDX, TGA, Mapping, ICP and VSM analysis were used to characterize and establish the structure of the heterogeneous nanocatalyst.

FT-IR analysis

The infrared spectra of pure Fe₃O₄ (a), Fe₃O₄@SiO₂ (b), Fe₃O₄@SiO₂@CPTES (c), Schiff base (d), Fe₃O₄@SiO₂@CPTES@ Schiff base (e) and Fe₃O₄@SiO₂@CPTES@Cu (II) Schiff base complex NPs (f) are illustrated in Fig. 1. The peak at 582 cm⁻¹ in Fig. 1a was observed, corresponding to the Fe–O vibration at the magnetite phase. The Si–O absorption appearing at 1087 cm⁻¹ confirms the successful functionalization of the Fe₃O₄ with tetraethyl orthosilicate (Fig. 1b). A new peak emerges at 2291 cm⁻¹ corresponding to CH₂ characteristic stretching band of the Fe₃O₄@SiO₂@CPTES (see Fig. 1c), indicating that the chloro-functional groups are successfully grafted onto the surface of the magnetic Fe₃O₄@SiO₂ NPs. There is a sharp band in 1621, 1580 cm⁻¹, attributed to C=N, indicating that Schiff base condensation has occurred (see Fig. 1d). Also, the absorption band at about 1620 cm⁻¹ is assigned that the Schiff base functional groups are successfully immobilized on the surface of the magnetic Fe₃O₄@SiO₂@CPTES NPs (Fig. 1e). The C=N band

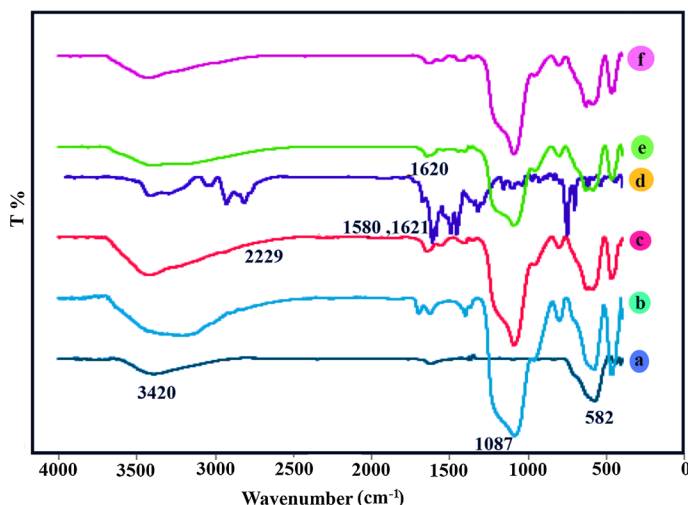


Fig. 1 FT-IR spectra of **a** naked Fe_3O_4 , **b** $\text{Fe}_3\text{O}_4@\text{SiO}_2$, **c** $\text{Fe}_3\text{O}_4@\text{SiO}_2@\text{CPTES}$, **d** ligand-Schiff base, **e** $\text{Fe}_3\text{O}_4@\text{SiO}_2@\text{CPTES}@\text{Schiff base}$ **f** $\text{Fe}_3\text{O}_4@\text{SiO}_2@\text{CPTES}@\text{Cu (II) Schiff base complex}$

shifts to a lower frequency in the spectrum 1f and deduces successful complexation of Schiff base to Copper (II) ion.

XRD analysis

X-ray diffraction (XRD) patterns of Fe_3O_4 and $\text{Fe}_3\text{O}_4@\text{SiO}_2@\text{CPTES}@\text{Cu (II) Schiff base complex}$ NPs separately are identified in Fig. 2. The obtained comparison results of XRD indicated that the crystalline structure of the Fe_3O_4 is still maintained after each of immobilization steps (Fig. 2b). The peaks located at the 2θ values of 31.13, 35.69, 43.15, 52.61, 57.11 and 62.78 are attributed to novel nano-catalyst.

Elemental analysis of the catalyst by EDS and ICP

Using the energy-dispersive X-ray spectroscopy (EDS) analysis, all related components of the nano-catalyst including Si, C, O, Fe, Cu, N and Cl are observed (Fig. 3) and proved that silica and organic layers are successfully loaded onto surface Fe_3O_4 nanoparticles. Besides, ICP-OES analysis of the catalyst specified that the weight percentage of Cu is 10.13%.

Scanning electron microscopy, transmission electron microscopy and mapping analysis

The structural formation of the nano-catalyst was investigated using SEM, TEM and mapping techniques discretely (Fig. 4). In the SEM image, Fig. 4a shows SEM

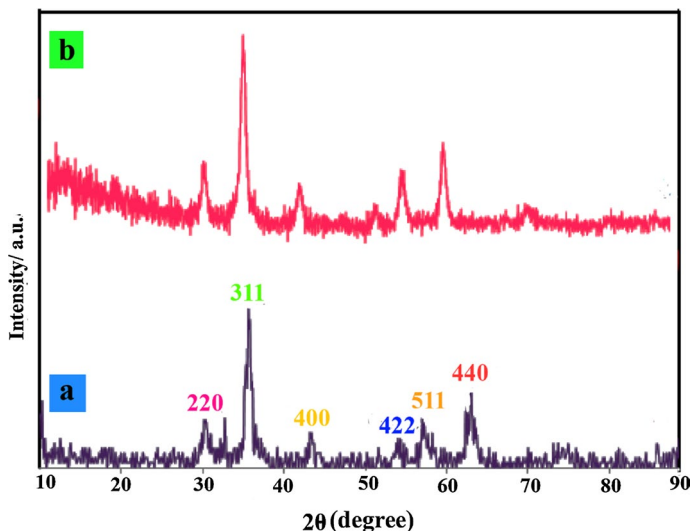


Fig. 2 XRD patterns of **a** naked Fe_3O_4 MNPs and **b** $\text{Fe}_3\text{O}_4@SiO_2@CPTES@Cu(II)$ Schiff base complex

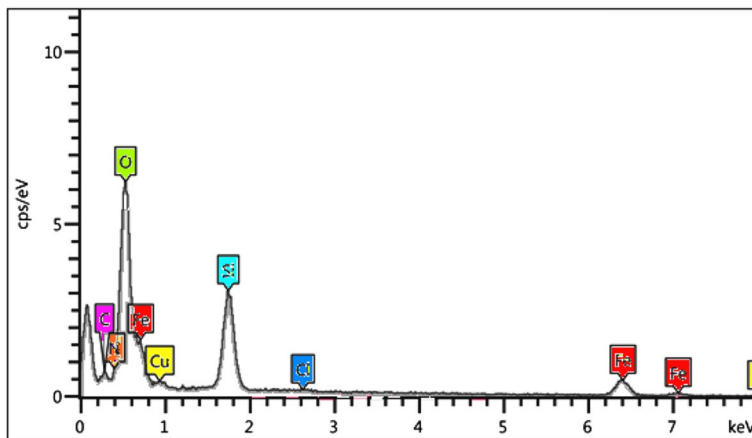


Fig. 3 The energy dispersive X-ray (EDX) spectrum of $\text{Fe}_3\text{O}_4@SiO_2@CPTES@Cu(II)$ Schiff base complex

images of surface morphology of the nano-catalyst that the average size of these MNPs is estimated to be about 40 nm. In the TEM image (Fig. 4b), there can be seen various layers coated on the surface of the Fe_3O_4 nanoparticles. Furthermore, the mapping image confirms the uniform distribution of these elements in the catalyst structure (Fig. 4c).

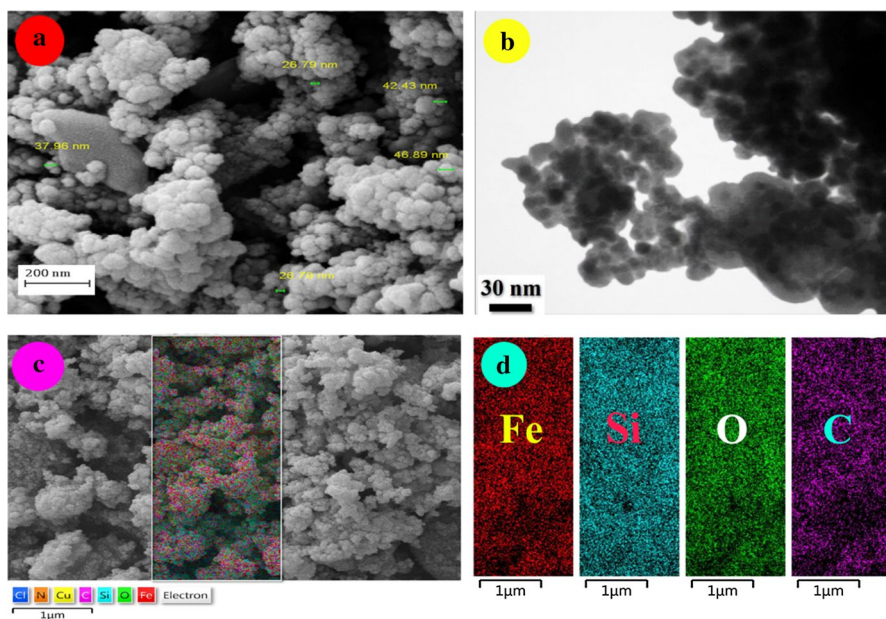


Fig. 4 **a** SEM, **b** TEM and **c** mapping images of the $\text{Fe}_3\text{O}_4@\text{SiO}_2@\text{CPTES}@\text{Cu (II)}$ Schiff base complex

Vibrating-sample magnetometer (VSM) analysis

The magnetic behavior of the Fe_3O_4 nanoparticles and the navel nano-catalyst is shown in Fig. 5. The magnetization curves of Fe_3O_4 (Fig. 5a) and the navel nano-catalyst (Fig. 5b) were found at 60 and 42 emu/g, separately. The observed results elucidated that the magnetization value of Fe_3O_4 was lower than that of navel nano-catalyst, due to the presence of silica-coated and surrounding Fe_3O_4 -nanoparticles cores.

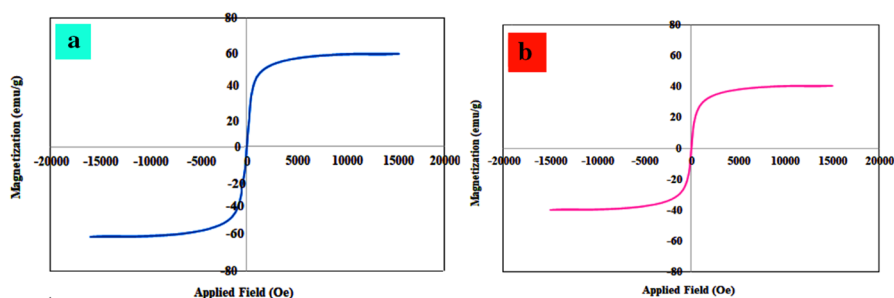


Fig. 5 Magnetization curves of **a** bare Fe_3O_4 and **b** $\text{Fe}_3\text{O}_4@\text{SiO}_2@\text{CPTES}@\text{Cu (II)}$ Schiff base complex

Thermogravimetric analysis (TGA-DTA)

The thermogravimetric analysis (TGA) was carried out from room temperature to 800 °C under atmosphere (Fig. 6) to investigate the thermal stability of the synthesized nano-catalyst. According to the TGA curve, the initial weight loss was observed at temperatures below 150 °C could be due to the adsorbed solvent or removal adsorbed water from the nano-catalyst. A further decrease in weight approximately 12% occurred between 250 and 429 °C which can be attributed to loss and decompose of the organic groups on Fe₃O₄ surface. According to these results, it can be concluded that adequate thermal stability for catalysis applications is up to 250 °C.

Evaluation of the catalytic activity and recyclability of the Copper nano-catalyst in the multicomponent synthesis via one-pot reaction

After the design, synthesis and characterization of the nano-catalyst, we used the nano-catalyst in the one-pot synthesis of 5-oxo-dihydropyrano[3,2-*c*] chromene, 2-amino-3-cyano-1,4,5,6-tetrahydropyrano[3,2-*c*] quinolin-5-one and 1*H*-pyrazolo[1,2-*b*]phthalazine-5,10-dione derivatives using the reaction between various aldehydes, 4-hydroxycoumarin/4-hydroxyquinolin-2(1*H*)-one/phthalhydrazide and malononitrile (Scheme 3). Initially, a mixture of benzaldehyde

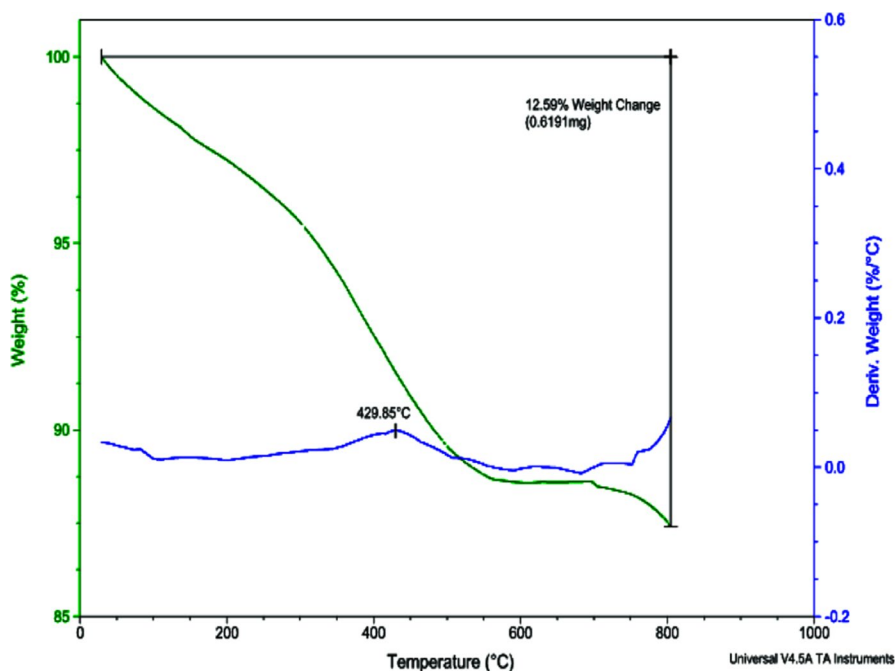
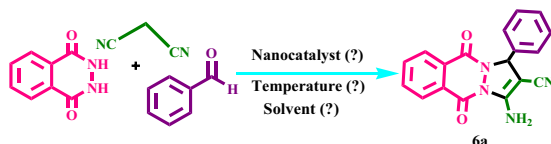


Fig. 6 TGA-DTG curve of Fe₃O₄@SiO₂@CPTES@Cu (II) Schiff base complex MNPs

(1 mmol), 4-hydroxycoumarin (1 mmol) and malononitrile (1 mmol) was selected as a model reaction. Consequently, the influence of parameters such as catalyst concentration, solvent and temperature was studied meticulously to achieve the best reaction conditions. According to Table 1, the obtained results have shown that the best conditions were carried out at 80 °C under the solvent-free condition with using 30 mg of the nano-catalyst (Table 1, entry 12). Thus, optimized reaction conditions with other aromatic aldehydes conducted were also similarly effective (Table 2). All reactions were completed within 10–15 min and given excellent isolated yields of products 4a–k. Similarly, to evaluate the best conditions for the synthesis of 3-amino-5,10-dihydro-5,10-dioxo-1-phenyl-1*H*-pyrazolo[1,2-*b*]phthalazine-2-carbonitrile, hereby the reaction was examined between benzaldehyde, malononitrile and phthalhydrazide as model reaction under conditions such as refluxing and stirring under various temperatures with different solvents (EtOH, H₂O, CH₃CN) or solvent-free conditions using various amounts of the nano-catalyst (Table 3). The model reaction was conducted with 30 mg of the nano-catalyst at 80 °C for 10 min and furnished 6a with a 97% yield. Encouraged by these results, it was remarkably realized and approved the important role of the nano-catalyst in this reaction by conducting the reaction in the absence of the catalyst that obtained in no detectable

Table 3 Optimization reaction for the synthesis of 1*H*-pyrazolo[1,2-*b*]phthalazine-5,10-dione derivatives



Entry	Catalyst amount (mg)	Solvent	Temperature (°C)	Time (min)	Yield ^a
1	No catalyst	H ₂ O	25	120	–
2	0.01	H ₂ O	25	120	30
3	0.01	EtOH	25	90	35
4	0.01	CH ₃ CN	25	60	50
5	0.01	Solvent-free	25	50	65
6	0.01	H ₂ O	Reflux	60	45
7	0.01	EtOH	Reflux	60	62
8	0.01	CH ₃ CN	Reflux	60	68
9	0.01	Solvent-free	70	40	72
10	0.01	Solvent-free	100	40	80
11	0.02	Solvent-free	80	10	95
12	0.03	Solvent-free	80	10	97
13	0.04	Solvent-free	70	10	85

Reaction Condition: benzaldehyde (1 mmol), phthalhydrazide (1 mmol), malononitrile (1 mmol), solvent (5 ml), ^aIsolated yields

amount of the product after a prolonged reaction time (Table 3, entry 1). Moreover, the catalytic activity of the Fe₃O₄@SiO₂@CPTES@Cu(II) Schiff base nanoparticles was compared with the catalytic activities of the bare Fe₃O₄, Fe₃O₄@SiO₂ and Fe₃O₄@SiO₂@CPTES supported Schiff base nanoparticles in separate experiments conducted under the same optimal conditions. The resulting yields given in Table 4 clearly indicated that the Fe₃O₄@SiO₂@CPTES@Cu(II) Schiff base nanoparticles perform relatively higher catalytic activity compared with other three nanoparticles.

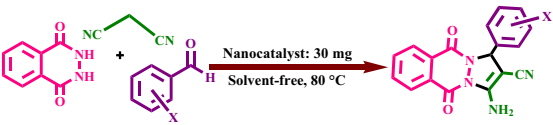
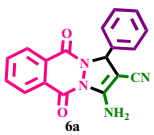
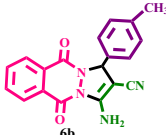

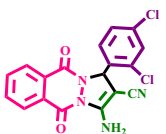
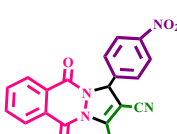
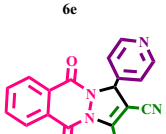
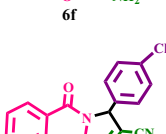
To expand the scope of this reaction, the variability of the aromatic aldehydes was also synthesized in good yields and the short time that the results summarized in Table 5. finally, Benzaldehyde derivatives such as 2,4-Cl, 3-NO₂, 4-C₅H₅N and 4-Cl-benzaldehyde undergo the reaction more readily than the aldehydes carrying electron-donating groups and afforded the desired products (6d–6 g) in very good yields relatively (Table 5). All the synthesized molecules are known compounds which were characterized using the usual spectroscopic techniques and compared with the data reported in the literature and the experimental section supported our spectroscopic data for some selected products. Since catalyst recovery and recyclability are remarkable and important for industrial and commercial applications as well as in green chemistry. Therefore, reusability and recovery of this nano-catalyst were investigated in the reaction of benzaldehyde (1 mmol), malononitrile (1 mmol), 4-hydroxycoumarin/ phthalhydrazide (1 mmol) and nano-catalyst (30 mg) at 80 °C under solvent-free (under optimized conditions). At the end of the reaction, the catalyst was magnetically removed the reaction mixture and separated with the help of an external magnet, washed with hot ethanol and dried. The nano-catalyst was reused for six runs. The obtained results (FT-IR, EDX, XRD of reused catalyst in the sixth run) had no distinct change in the structure and activity of the nano-catalyst (Fig. 7).

Investigation of catalyst recyclability in the synthesis of 4a (I), 6a (II) under optimized conditions.

Table 4 Comparative catalytic activity of Fe₃O₄@SiO₂@CPTES@ Cu(II) Schiff base nanoparticles under optimal conditions

Entry	Catalyst	Time (min)	Yield (%)
1	Fe ₃ O ₄ @SiO ₂ @CPTES@Cu(II) Schiff base	10	98
2	Fe ₃ O ₄ @SiO ₂ @CPTES@Schiff base	30	80
3	Fe ₃ O ₄ @SiO ₂	120	58
4	Fe ₃ O ₄	35	70

Table 5 Fe₃O₄@SiO₂@CPTES@Cu (II) Schiff base complex catalyzed synthesis of 1*H*-pyrazolo[1,2-*b*]phthalazine-5,10-dione derivatives

					
Entry	X	Product	Time (min)	Yield ^a (%)	M.P (°C) [Lit.] [59–62]
1	H	 6a	10	97	272–274
2	4-CH ₃	 6b	15	90	256–258
3	4-OCH ₃	 6c	15	92	240–242
4	2,4-Cl ₂	 6d	10	98	246–248
5	4-NO ₂	 6e	10	95	256–258
6	4-C ₅ H ₄ N	 6f	15	96	260–262
7	4-Cl	 6g	10	96	270–272

Conditions: aldehyde (1 mmol), malononitrile (1 mmol), phthalhydrazide (1 mmol), catalyst (30 mg), 80 °C, ^aIsolated pure yield

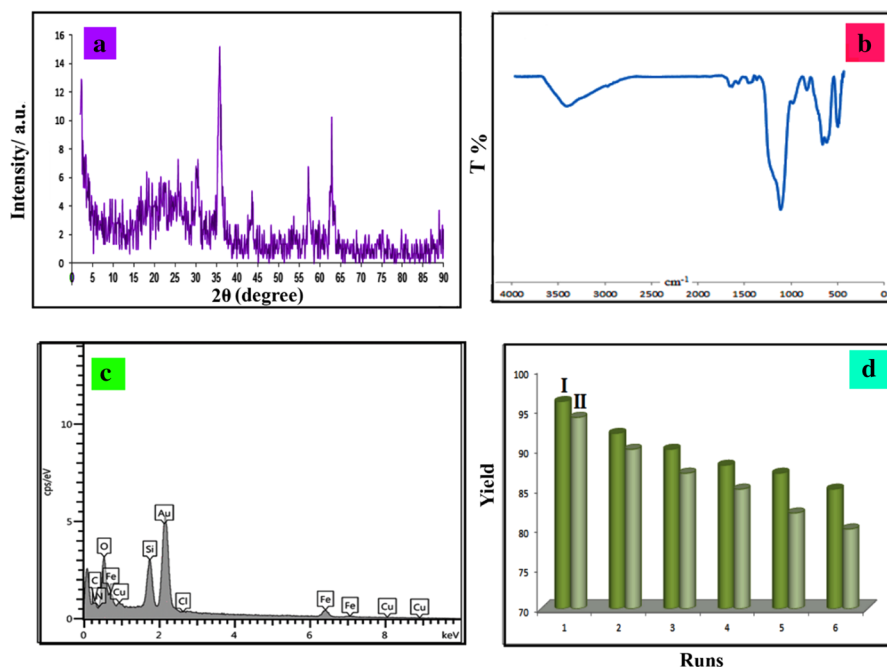
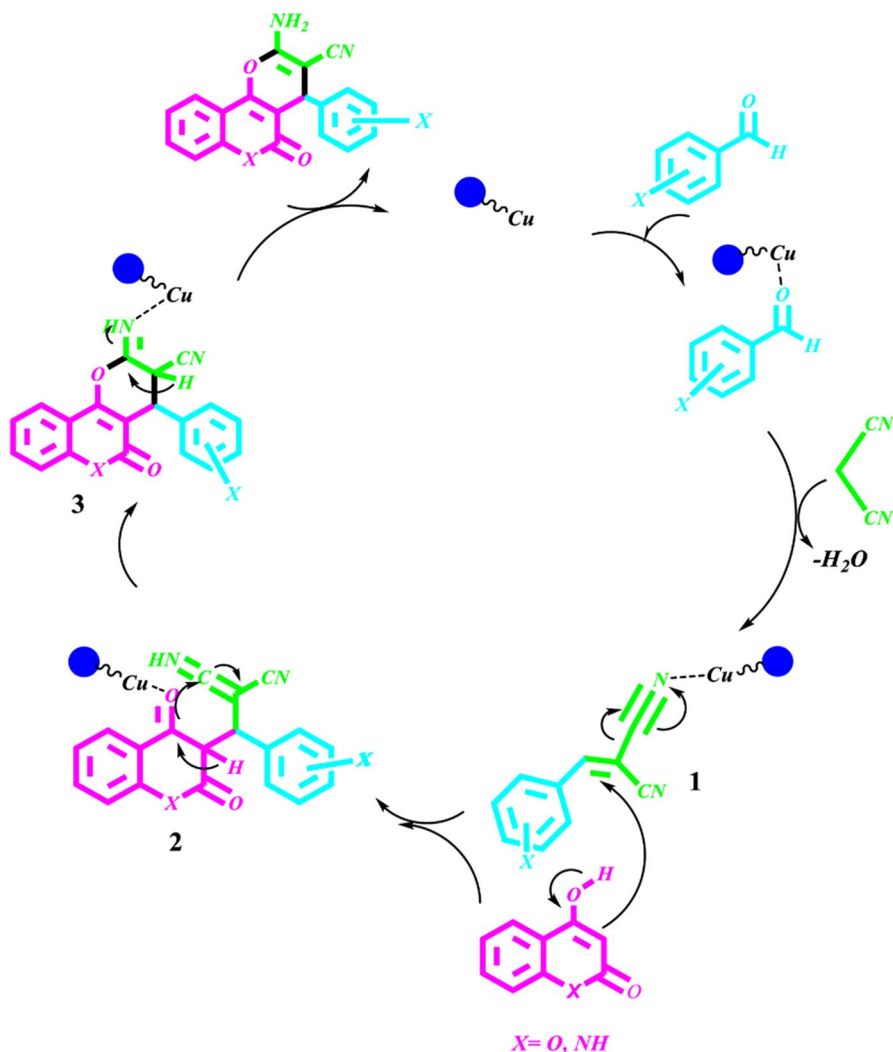


Fig. 7 **a** The XRD of reused catalyst, **b** the FT-IR reused catalyst, **c** the EDX of reused catalyst and **d** Recyclability of the catalyst in synthesis of 4a (I), 6a (II) under the optimized conditions

Proposed reaction mechanism

A plausible mechanism for synthesis of 5-oxo-dihydropyrano[3,2-*c*]chromene, 2-amino-3- cyano-1,4,5,6-tetrahydropyrano[3,2-*c*] quinolin-5-one derivatives

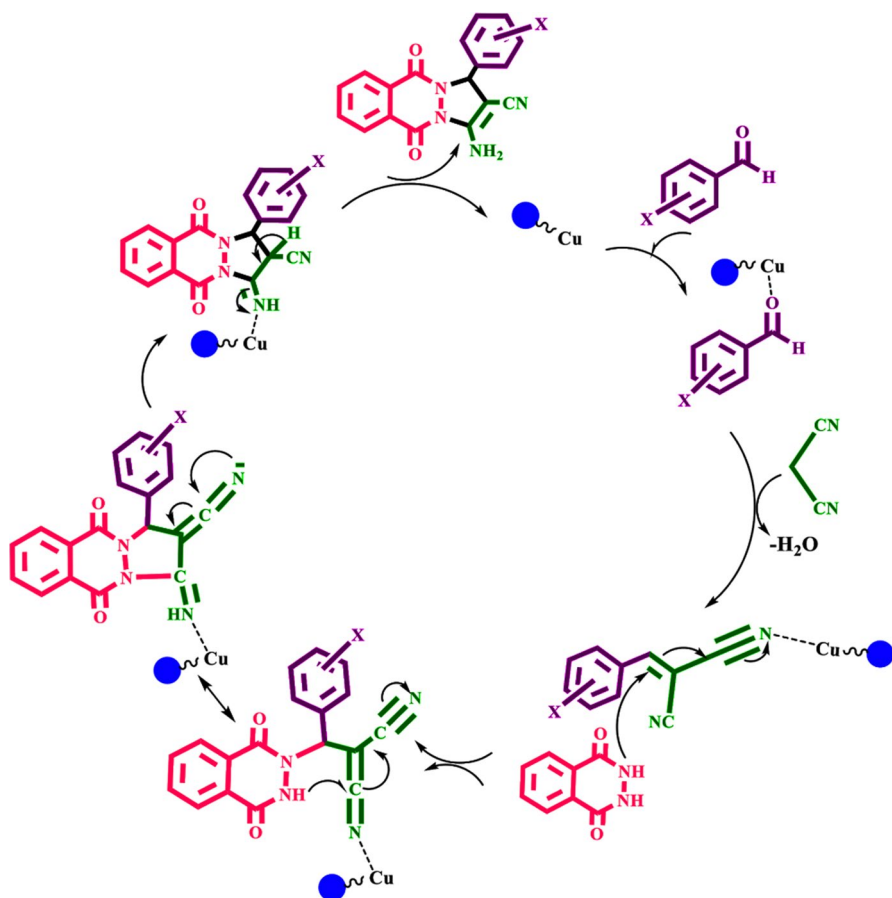
Scheme 4 shows a plausible mechanism for the synthesis of 5-oxo-dihydropyrano[3,2-*c*]chromene, 2-amino-3-cyano-1,4,5,6-tetrahydropyrano[3,2-*c*] quinolin-5-one derivatives catalyzed by $\text{Fe}_3\text{O}_4@\text{SiO}_2@\text{CPTES}@\text{Cu}$ (II) Schiff base complex NPs. In first, the aromatic aldehyde is activated by the nano-catalyst. So that, activated aldehyde reacts with malononitrile via a Knoevenagel condensation reaction and products the intermediate (1). Next, 4-hydroxycoumarin/4-hydroxyquinolin-2(1*H*)-one adds to the intermediate (1) to generate the Michael adduct (2) by the nano-catalyst. Finally, enolization of (II) occurs to yield the intermediate (3) which undergoes intramolecular nucleophilic cyclization to provide highly respective products 4(a-k) [53].



Scheme 4 Proposed mechanism for Fe₃O₄@SiO₂@CPTES@Cu (II) Schiff base complex catalyzed synthesis of 5-oxo-dihydropyrano[3,2-*c*]chromene-2-amino-3-cyano-1,4,5,6-tetrahydropyrano- [3,2-*c*]quino- lin-5-one derivatives

Plausible mechanism for synthesis of 1H-pyrazolo[1,2-*b*]phthalazine-5,10-dione derivatives

Based on a literature survey [60], a similar plausible mechanism synthesis of 1H-pyrazolo[1,2-*b*]phthalazine-5,10-dione derivatives 6(a-g) is shown in Scheme 5. The first step involves the formation of ylidene malononitrile via the condensation of aromatic aldehydes with malononitrile under the catalytic effect of the nano-catalyst (Intermediate 1), Then, Michael addition between intermediate (1) and



Scheme 5 Proposed mechanism for $\text{Fe}_3\text{O}_4@\text{SiO}_2@\text{CPTES}@\text{Cu}(\text{II})$ Schiff base complex catalyzed synthesis of 1H-pyrazolo[1,2-b]phthalazine-5,10-dione derivatives

phthalhydrazide, followed by intramolecular cyclization, is assisted the nano-catalyst to furnish the desired pure products.

Conclusion

In summary, we designed and synthesized a copper/Schiff base complex immobilized on silica MNPs as a novel nanomagnetic catalyst and characterized by diverse analytical techniques. This nanoparticle has been introduced as an efficient and green protocol for the one-pot synthesis of dihydropyrano[3,2-c]chromen-2-one, 2-amino-3-cyano-1,4,5,6-tetrahydropyrano[3,2-c]quinolin-5-one and 1H-pyrazolo[1,2-b]phthalazine-5,10-dione derivatives. The main advantages of this catalytic method are high yields of products, short reaction times, high surface area, thermal stability,

the use of an inexpensive copper metal and the simple of separation without the need for column chromatographic, recovery, reuse and eco-friendliness of the nano-catalyst. Besides, the catalyst is reusable and shows efficiency up to 6 cycles without significant loss of the catalytic activity or metal loading. We anticipate from the strategy in our work can provide an attractive catalytic system large-scale degradation of organic pollutants and other industrially significant products.

Acknowledgements The authors wish to thank the Research Council of Bu-Ali Sina University for financial support to carry out this research.

Compliance with ethical standards

Conflicts of interest We have no conflicts of interest to disclose.

References

1. S. Chandra, L.K. Gupta, S. Agrawal, *Trans. Met. Chem.* **32**, 240 (2007)
2. A.I. Hanafy, A.B.K.T. Maki, M.M. Mostafa, *Trans. Met. Chem.* **32**, 960 (2007)
3. S. Chandra, A. Gautum, M. Tyagi, *Trans. Met. Chem.* **32**, 1079 (2007)
4. L.T. Bozic, E. Marotta, P. Traldi, *Polyhedron* **26**, 1663 (2007)
5. H. Keypour, M. Shayesteh, M. Rezaeivala, F. Chalabian, Y. Elerman, O. Buyukgungor, *J. Mol. Str.* **1032**, 62 (2013)
6. S. Ilhan, H. Temel, *Trans. Met. Chem.* **32**, 1039 (2007)
7. M.C. Fernandez, R. Basitida, A. Macias, L. Valencia, P.P. Lourida, *Polyhedron* **25**, 783 (2006)
8. S. Mahmoudi-GomYek, D. Azarifar, M. Ghaemi, H. Keypour, M. Mahmoudabadi, *Appl. Organometal. Chem.* **33**, e4918 (2019)
9. X. Wu, C. Lu, Z. Zhou, G. Yuan, R. Xiong, X. Zhang, *Environ. Sci. NANO* **1**, 71 (2014)
10. H. Ebrahimiasl, D. Azarifar, *Appl. Organometal. Chem.* **34**, e5359 (2020)
11. L. Ma'mani, M. Sheykhan, A. Heydari, M. Faraji, Y. Yamini, *Appl. Catal. A* **250**, 64 (2010)
12. J. Deng, L.P. Mo, F.Y. Zhao, L.L. Hou, L. Yang, Z.H. Zhang, *Green Chem.* **254**, 2576 (2011)
13. A. Saxena, A. Kumar, S. Mozumdar, *J. Mol. Catal. A: Chem.* **269**, 35 (2007)
14. C. Yuan, Z. Huang, J. Chen, *Catal. Commun.* **24**, 56 (2012)
15. Z. Cimerman, S. Miljanić, N. Galić, *Croat. Chem. Acta* **73**, 81 (2000)
16. D.N. Dhar, C.L. Taploo, *J. Sci. Indust. Res.* **41**, 501 (1982)
17. B.S. Sathe, E. Jaychandran, V.A. Jagtap, G.M. Sreenivasa, *Inter. J. Pharm. Res. Dev.* **3**, 164 (2011)
18. A. Pandey, D. Dewangan, S. Verma, A. Mishra, R.D. Dubey, *Inter. J. ChemTech Res.* **3**, 178 (2011)
19. C. Chandramouli, M.R. Shivanand, T.B. Nayanbhai, B. Bheemachari, R.H. Udipi, *J. Chem. Pharm. Res.* **4**, 1151 (2012)
20. S. Li, S. Chen, S. Lei, H. Ma, R. Yu, D. Liu, *Corros. Sci.* **41**, 1273 (1999)
21. P. Venkatesh, *Asian J. Pharm. Health Sci.* **1**, 8 (2011)
22. A.K. Chaubey, S.N. Pandeya, *Inter. J. ChemTech Res.* **4**, 590 (2012)
23. K. Mounika, B. Anupama, J. Pragathi, C. Gyanakumari, *J. Sci. Res.* **2**, 513 (2010)
24. R. Miri, N. Razzaghi-asl, M. K. Mohammadi, *J. Mol. Model.*, **19**, 727 (2013).
25. D. Wei, N. Li, G. Lu, K. Yao, *Sci. China B* **49**, 225 (2006)
26. G. Avaji, C. H. Vinod Kumar, S. A. Patil, K. N. Shivananda, *Eur. J. Med. Chem.*, **44**, 3552 (2009).
27. T. Aboul-Fadl, F.A. Mohammed, E.A. Hassan, *Arch. Pharm. Res.* **26**, 778 (2003)
28. S. Chandra, M. Pundir, *Spectrochim. Acta A* **69**, 1 (2008)
29. S. Chandra, R. Gupta, N. Gupta, S.S. Bawa, *Trans. Met. Chem.* **31**, 147 (2006)
30. S. Chandra, L.K. Gupta, S. Agrawal, *Trans. Met. Chem.* **32**, 558 (2007)
31. G. Cerchiaro, A.M.C. Ferreira, *J. Braz. Chem. Soc.* **17**, 1473 (2006)
32. M. B. Gawande, A. Goswami, F.-X. Felpin, T. Asefa, X. Huang, R. Silva, X. Zou, R. Zboril, R. S. Varma, *Chem. Rev.*, **116**, 6, 3722 (2016).
33. D. Das, *Chem. Select.*, **1**, 9, 1959 (2016).

34. I. Bertini-H.B. Gray-S.J. Lippard-J.S. Valentine, Bioinorganic chemistry, University Science Books, 1994.
35. M. Norouzi, A. Ghorbani-Choghamarani, M. Nikoorazm, RSC Adv. **6**, 92387 (2016)
36. H. Keypour, M. Rezaeivala, L. Valencia, P. Pérez-Lourido, H.R. Khavasi, Polyhedron **28**, 3755 (2009)
37. N. Raman, Y. P. Raja, A. Kulandaisamy, J. Chem. Sci., **11**, 183 (2001).
38. S. Sobhani, F. Khakzad, Appl. Organomet. Chem. **31**, e3877 (2017)
39. A. Ghorbani-Choghamarani, B. Tahmasbi, P. Moradi, N. Havasi, Appl. Organomet. Chem. **30**, 619 (2016)
40. M. Hajjami, S. Kolivand, Appl. Organomet. Chem. **30**, 282 (2016)
41. R. Zahedi, Z. Asadi, F.D. Firuzabadi, A Highly Active, Cat. Lett., **1** (2019).
42. J. Zhu-H. Bienaymé, *Multicomponent reactions*, Wiley, New York, 2006.
43. H. Bienaymé, C. Hulme, G. Oddon, P. Schmitt, Chem-Eur. J. **6**, 3321 (2000)
44. R.V. Orru, E. Ruijter, *Synthesis of heterocycles via multicomponent reactions II*, Springer Science & Business Media, Heidelberg, 2010.
45. M. Khaleghi-Abbasabadi, D. Azarifar, Res. Chem. Intermed. **45**, 2095 (2019)
46. D. Azarifar, O. Badalkhani, Y. Abbasi, M. Hasanabadi, J. Iran. Chem. Soc. **14**, 403 (2017)
47. M. Piltan, Heterocyclic Commun. **2**, 401 (2017)
48. M.-J. Yao, Z. H. Guan, Y. He, Synth. Commun. **43**, 2073 (2013)
49. H. Keypour, M. Aidi, M. Mahmoudabadi, R. Karamian, M. Asadbeg, R.W. Gable, J. Mol. Struct. **1198**, 126666 (2019)
50. M. Ma, Y. Zhang, X. Li, D. Fu, H. Zhang, N. Gu, Colloids Surf. A. Physicochem. Eng. Asp. **224**, 207 (2003)
51. M. Tajbakhsh, M. Farhang, R. Hosseinzadeh, Y. Sarrafi, RSC Adv. **4**, 23116 (2014)
52. D. Azarifar, H. Ebrahimiasl, R. Karamian, M. Ahmadi-Khoei, J. Iran. Chem. Soc. **16**, 341 (2019)
53. K. Tabatabaiean, H. Heidari, M. Mamaghani, N.O. Mahmoodi, Appl. Organomet. Chem. **26**, 56 (2012)
54. M. Khoobi, L. Ma'mani, F. Rezazadehb, Z. Zareieb, A. Foroumadi, A. Ramazanib, J. Mol. Catal. A Chem. **359**, 74 (2012).
55. D. Azarifar, O. Badalkhani, Y. Abbasi, M. Hasanabadi, J. Iran. Chem. Soc. **14**, 403 (2017)
56. K. Niknam, A. Piran, Curr. Opin. Green Sustain. Chem. **3**, 1 (2013)
57. E. Abbaspour-Gilandeh, M. Aghaei-Hashjinb, A. Yahyazadeh, H. Salemi, RSC Adv. **6**, 55444 (2016)
58. M. Lei, L. Ma, L.H. Hu, Tetrahedron Lett. **52**, 2597 (2011)
59. R. Ghahremanzadeh, Gh Imani Shakibaei, A. Bazgir, Synlett, 1129 (2008).
60. M.R. Nabid, S.J. Tabatabaei Rezaei, R. Ghahremanzadeh, A. Bazgir, Ultrason. Sonochem., **17**, 159 (2010).
61. A. Vafaei, A. Davoodnia, M. Pordel, M.R. Bozorgmehr, Orient. J. Chem. **31**, 2153 (2015)
62. A. Mulika, M. Deshmukha, D. Chandama, P. Patilb, S. Jagdalea, D. Patila, S. Sankpal, Der Pharma. Chem. **5**, 19 (2013)

Publisher's Note Springer Nature remains neutral with regard to jurisdictional claims in published maps and institutional affiliations.